V. Conclusion

Since the wavelet transform is actually the constant-Q special case of the generalized short-time Fourier transform, results which apply to the GSTFT can also be applied to the WT. The wavelet magnitude analysis theorem is one specific example of how (preexisting) GSTFT research can be beneficially applied to wavelet analysis. The theorem shows that scalograms are similar to analysis by a particular type of filter/detector bank. As a consequence, it is possible to define appropriate scalogram sampling rates for computation and data reduction purposes. Other GSTFT results which predate wavelet analysis can also be applied, thereby accelerating the development of wavelet theory as a field of study.

References

[1] L. R. Rabiner and R. W. Schafer, *Digital Processing of Speech Signals*. Englewood Cliffs, NJ: Prentice-Hall, 1978, Sec. 6.1.4 and Prob. 6.6.

[2] J. C. Anderson, "A filter/detector interpretation of the short-time Fourier transform magnitude," in *Proc. ICASSP'85* Tampa, FL, Mar. 26-29 1985, pp. 533-536.

[3] O. Rioul and M. Vetterli, "Wavelets and signal processing," *IEEE Signal Processing Mag.*, vol. 8, pp. 14-38, Oct. 1991.

[4] J. C. Anderson and C. L. Searle, "Speech analysis/synthesis based on perception," in *Proc. ICASSP'83*, Boston, MA, Apr. 14-16, 1983, pp. 1364-1367.

[5] J. C. Anderson, "A spectral magnitude analysis theorem and applications," in *IEEE Signal Processing. Symp. Time-Frequency Time-Scale Anal.*, Victoria, B.C., Canada, Oct. 4-6, 1992, pp. 277-280.

[6] —, "Speech analysis/synthesis based on perception," Ph.D. dissertation, Dept. Elec. Eng. & Comput. Sci., Mass. Inst. Tech., Cambridge MA, MIT Lincoln Lab. Tech. Rep. 707, ESD-TR-84-048, DTIC #AD-A151320/9/XAB, 1984.

[7] A. V. Oppenheim and A. S. Willsky (with I. T. Young), *Signals and Systems*. Englewood Cliffs, NJ: Prentice-Hall, 1983.

[8] J. Morlet, G. Arens, E. Fourgeau, and D. Giard, "Wave propagation and sampling theory—part II: Sampling theory and complex waves," *Geophysics*, vol. 47, pp. 222-236, Feb. 1982.

[9] R. P. Lippmann, L. D. Braida, and N. I. Durlach, "Study of multichannel amplitude compression and linear amplification for persons with sensorineural hearing loss," *J. Acoust. Soc. Amer.* vol. 69, pp. 524-534, Feb. 1981.

[10] T. Irino and H. Kawahara, "Signal Reconstruction from Modified Wavelet Transform: An Application to Auditory Signal Processing," in *Proc. ICASSP'92*, San Francisco CA, Mar. 23-26, 1992, pp. I85-88.

Shear Madness: New Orthonormal Bases and Frames Using Chirp Functions

Richard G. Baraniuk and Douglas L. Jones

***Abstract*—The proportional-bandwidth and constant-bandwidth time-frequency signal decompositions of the wavelet, Gabor, and Wilson orthonormal bases have attracted substantial interest for representing nonstationary signals. However, these representations are limited in that they are based on rectangular tessellations of the time-frequency plane. While much effort has gone into methods for designing nice wavelet and window functions for these frameworks, little consideration has been given to methods for constructing orthonormal bases employing *nonrectangular* time-frequency tilings. In this note, we take a first step in this direction by deriving two new families of orthonormal bases and frames employing elements that shear, or chirp, in the time-frequency plane, in addition to translate and scale. The new scale-shear *fan* bases and shift-shear *chevron* bases are obtained by operating on an existing wavelet, Gabor, or Wilson basis set with two special unitary warping transformations. In addition to the theoretical benefit of broadening the class of valid time-frequency plane tilings, these new bases could possibly also be useful for representing certain types of signals, such as chirping and dispersed signals.**

Manuscript received August 21, 1992; revised May 26, 1993. The Guest Editor coordinating the review of this paper and approving it for publication was Dr. Patrick Flandrin. This work was supported in part by the Sound Group of the computer-based Education Research Laboratory, University of Illinois, in part by an NSERC-NATO postdoctoral fellowship, in part by the Joint Services Electronics Program under Grant N00014-90-J-1270, and in part by the National Science Foundation under Grant MIP 90-12747.

R. G. Baraniuk is with the Department of Electrical and Computer Engineering, Rice University, Houston, TX 77251-1892.

D. L. Jones is with the Coordinated Science Laboratory, University of Illinois, Urbana, IL 61801.

IEEE Log Number 9212184.

I. Introduction

The continuous wavelet transform and the short-time Fourier transform are multidimensional functionals that map one-dimensional signals to the two-dimensional time-frequency plane [1]. Both have been utilized in numerous signal processing applications to analyze the time-varying frequency content of nonstationary signals.

Attention has focused recently on using these transforms to construct orthonormal bases and frames for the signal space of square-integrable functions $L^2(\mathbb{R})$.[1] A function (or signal) s from $L^2(\mathbb{R})$ can be represented in terms of a doubly-indexed, orthonormal basis set $\{\boldsymbol{b}_{m,n}\}$ using[2]

$$s = \sum_{m,n} c_{m,n}\boldsymbol{b}_{m,n}. \tag{1}$$

Each expansion coefficient $c_{m,n}$ is computed by projecting the signal onto the corresponding basis element; that is $c_{m,n} = \langle s, \boldsymbol{b}_{m,n}\rangle$, where $\langle f, g\rangle = \int f(u)g^*(u)\,du$ denotes the inner product for $L^2(\mathbb{R})$.

The elements of a wavelet basis are obtained by translating and scaling a single nonarbitrary but fixed wavelet function g_{wavelet}

$$\boldsymbol{b}_{m,n}^{\text{wavelet}}(t) = a_0^{-m/2} g_{\text{wavelet}}(a_0^{-m}t - nt_0) \tag{2}$$

with $t_0a_0 = 2$ and $m, n \in \mathbb{Z}$. The basis elements can be interpreted as "tiling" the time-frequency plane in a proportional-bandwidth (constant-Q) fashion; the tiling for an identified wavelet basis is depicted in Fig. 1(a). A class of wavelets having both compact support and arbitrarily high *regularity* (smoothness) has been derived by Daubechies [4].

Short-time Fourier transform bases are often referred to as *Gabor* bases, because they share the same form as the seminal transform of Gabor [5]. The elements of a Gabor basis are obtained by translating and modulating a single nonarbitrary but fixed window function g_{Gabor}

$$\boldsymbol{b}_{m,n}^{\text{Gabor}}(t) = g_{\text{Gabor}}(t - nt_0)\exp(j2\pi mf_0t) \tag{3}$$

with $t_0f_0 = 1$ and $m, n \in \mathbb{Z}$. A Gabor basis tiles the time-frequency plane in a contant-bandwidth fashion; the tiling for an idealized basis is pictured in Fig. 1(b). Windows generating Gabor bases have been constructed by Balian [6], Jensen, Høholdt, and Justesen

[1] To be concrete, we will discuss only orthonormal bases for the Hilbert space $L^2(\mathbb{R})$ in this note. Note, however, that all results apply also to the more general frame case [2] and that many results can be extended to more general Banach spaces [3]. From this point on, we will also simply use the term *basis* to mean *orthonormal basis*.

[2] All sums and integrals are assumed to go from $-\infty$ to ∞ unless otherwise stated.

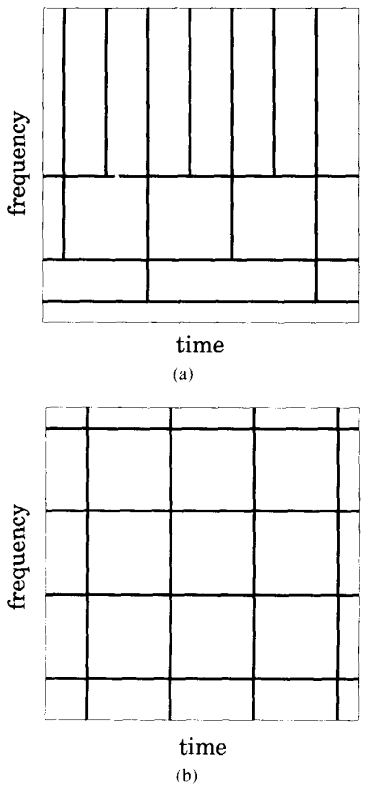

Fig. 1. Idealized tiling of the time–frequency plane by (a) the elements $\{\boldsymbol{b}_{m,n}^{\text{wavelet}}\}$ of a wavelet orthonormal basis and (b) the elements $\{\boldsymbol{b}_{m,n}^{\text{Gabor}}\}$ of a Gabor orthonormal basis.

[7], Tolimieri and Orr [8], and Coifman, Meyer, and Wickerhauser [9]. Recently, constant-bandwidth bases of the Wilson type have been proposed as a well-localized alternative to the Gabor bases [10].

With the wavelet, Gabor, and Wilson bases, we have two disparate tilings of the time-frequency plane, each of which is well suited for representing certain classes of signals. However, what if the signals we wish to decompose are not well modeled by either a proportional-bandwidth or a constant-bandwidth analysis? For example, the energy of a frequency modulated signal will be spread over many basis coefficients in both types of expansions, since it traces a path in the time-frequency plane that is not well modeled by either of the basis tilings shown in Fig. 1(a) or (b). Clearly, to best match signals of this sort, we must find more flexible bases whose elements are not restricted to a strictly rectangular geometry in the time-frequency plane.

While much effort has gone into methods for designing nice wavelet and window functions g for the wavelet, Gabor, and Wilson bases, little consideration has been given to methods for constructing orthonormal bases and frames employing nonrectangular, "non-Manhattan" tessellations of the time-frequency plane. In this correspondence, we take a first step in this direction and present two new families of orthonormal bases employing elements that *shear*, or chirp, in the time-frequency plane in addition to translate and scale. These new bases can be interpreted as generalizing the wavelet, Gabor, and Wilson basis constructions to allow chirping elements. Besides the theoretical benefit of expanding the class of time-frequency tilings available through current techniques, these new bases may produce better results (packing more energy into fewer expansion coefficients, for example) than existing bases for certain types of signals, since the chirping action can be used to better match the basis elements to these signals.

The remainder of this note is organized into two major sections, one for the generalization of the proportional-bandwidth (wavelet) bases and one for the generalization of the constant-bandwidth (Gabor, Wilson) bases. In Section II, we construct a special warping operator that remaps orthonormal wavelet bases into *fan* bases, whose elements scale and shear in the time-frequency plane. Then, in Section III, we apply a similar procedure to the Gabor and Wilson bases to yield two types of *chevron* bases, whose elements translate and shear in the time-frequency plane. Results on the regularity of these new basis constructions follow in Section IV. A discussion and conclusion are offered in the final section.

II. Generalized Wavelet Bases: The Fan Bases

A. Basis Elements

The key to the construction of the scale-shear fan bases is in the Fourier transform of a wavelet basis element:

$$\boldsymbol{B}_{m,n}^{\text{wavelet}}(f) = (\boldsymbol{F}\boldsymbol{b}_{m,n}^{\text{wavelet}})(f) = a_0^{m/2} G_{\text{wavelet}}(a_0^m f) \cdot \exp(-j2\pi n t_0 a_0^m f). \tag{4}$$

Here $\boldsymbol{F}$ denotes the Fourier transform operator and G_{wavelet} represents the Fourier transform of g_{wavelet}; we will use capital letters to denote the Fourier transforms of functions. Recall that a wavelet expansion is valid only for wavelets $g_{\text{wavelet}} \in L^2(\mathbb{R})$ that satisfy the admissibility condition

$$\int |G_{\text{wavelet}}(f)|^2 \frac{df}{|f|}. \tag{5}$$

This condition can also be expressed as $G_{\text{wavelet}} \in K_1(\mathbb{R})$, where $K_r(\mathbb{R})$ is the "weighted L^2" Hilbert space defined as

$$K_r(\mathbb{R}) = \left\{ z: \int |z(v)|^2 \frac{dv}{|v|^r} < \infty \right\}, \qquad r \in \mathbb{R}. \tag{6}$$

Note that $K_0(\mathbb{R}) = L^2(\mathbb{R})$.

The scale-shear fan bases are constructed simply by replacing the linear f terms in the exponential of (4) with another power of f:

$$\boldsymbol{B}_{m,n}^{\text{fan}}(f) = r_0^{m/2} G_{\text{fan}}(r_0^m f) \exp[-j2\pi n p_0 |r_0^m f|^c \operatorname{sign}(f)], \quad c \in \mathbb{R}, \; c \neq 0. \tag{7}$$

Taking the inverse Fourier transform of $\boldsymbol{B}_{m,n}^{\text{fan}}$ yields the proposed fan basis element of order c:

$$\boldsymbol{b}_{m,n}^{\text{fan}}(t) = (\boldsymbol{F}^{-1}\boldsymbol{B}_{m,n}^{\text{fan}})(t) = r_0^{-m/2}(\boldsymbol{C}_{np_0}^c g_{\text{fan}})(r_0^{-m}t). \tag{8}$$

Here the operator $\boldsymbol{C}_k^c$ represents convolution with a hyper-chirp function of order c and chirp rate k, that is

$$(\boldsymbol{C}_k^c g)(t) = (g * h_k^c)(t) \tag{9}$$

with

$$h_k^c(t) = (\boldsymbol{F}^{-1} \exp[-j2\pi k|f|^c \operatorname{sign}(f)])(t) = \int \exp[-j2\pi k|f|^c \operatorname{sign}(f)] e^{j2\pi ft}\, df. \tag{10}$$

Equation (8) indicates that the building blocks of a fan basis are obtained by convolving a fixed function g_{fan} with a chirp function of rate np_0 and then scaling the result. The chirp convolution causes

the basis elements to *shear* in the time direction in the time-frequency plane. Different values of the order parameter c correspond to different types of chirps and, hence, produce completely different time-frequency plane tilings: $c = 1$ yields the usual wavelet transform, $c = 2$ yields bases employing linear chirps, $c = 3$ yields bases employing parabolic chirps, and so on. The tiling for an idealized fan basis for the $c = 2$, linear chirp case is illustrated in Fig. 2. The tilt of the elements in the fan suggests that these bases could prove useful for representing linear chirp signals.

B. The Axis Warping Operator Λ_c

We now establish the validity of the proposed fan basis given in (8). Remarkably, a simple change of variable will yield all generalized wavelets g_{fan} that generate fan orthonormal bases.

Definition 1: The *axis warping operator* Λ_c on $L^2(\mathbb{R})$ is given by

$$(\Lambda_c z)(v) = |c|^{1/2}|v|^{(c-1)/2} z(|v|^c \text{ sign } (v)),$$
$$c \in \mathbb{R}, \; c \neq 0. \tag{11}$$

The inverse axis warping operator is

$$(\Lambda_c^{-1} z)(v) = |c|^{-1/2}|v|^{(1-c)/2c} z(|v|^{1/c} \text{ sign } (v)). \tag{12}$$

In this section, we will apply this warping operator to the Fourier transform of a wavelet basis element to construct a fan basis element. Note that Λ_c maps the complex Fourier-domain sinusoid $e^{j2\pi f}$ to the chirp function $\sqrt{|c|f|^{c-1}}$ exp $[j2\pi|f|^c \text{ sign } (f)]$. A fundamental property of the axis warping operator is that it is an isometric isomorphism from the space $K_r(\mathbb{R})$ onto $K_{cr}(\mathbb{R})$.[3]

Roughly speaking, if two vector spaces $\mathfrak{X}$ and $\mathfrak{Y}$ are isometrically isomorphic, then they are structurally equivalent in the sense that the points in $\mathfrak{Y}$ are simply relabeled versions of the points in $\mathfrak{X}$ (and vice versa). An isometric isomorphism T that links a space $\mathfrak{X}$ with itself, that is, T: $\mathfrak{X} \to \mathfrak{X}$, is termed *unitary*. A very important unitary operator is the Fourier transform, which maps $L^2(\mathbb{R})$ onto itself. We now state the key result of this section.

Theorem 1: The axis warping operator Λ_c is an isometric isomorphism from the Hilbert space $K_r(\mathbb{R})$ onto $K_{cr}(\mathbb{R})$ for all r, $c \in \mathbb{R}$, $c \neq 0$.

Proof: The linearity, isometry, and bijectivity of Λ_c are easily verified using the simple change of variable $u = |v|^c$ sign (v) in each case. □

Since the Fourier transform operator $\boldsymbol{F}$ is an isometric isomorphism from $L^2(\mathbb{R})$ onto $L^2(\mathbb{R})$, the three-part operator $\Theta_c = \boldsymbol{F}^{-1}\Lambda_c\boldsymbol{F}$ formed by composing $\boldsymbol{F}$ with the axis warping operator is also an isometric isomorphism. The following diagram summarizes an important set of spaces that are linked isometrically and isomorphically by these operators:

$$\mathfrak{A} \xrightarrow{\boldsymbol{F}} \hat{\mathfrak{A}} \subset K_1(\mathbb{R}) \xrightarrow{\Lambda_c} \hat{\mathfrak{B}} \subset K_c(\mathbb{R}) \xrightarrow{\boldsymbol{F}^{-1}} \mathfrak{B}. \tag{13}$$

The set $\mathfrak{A}$ signifies the set of all admissible wavelets in $L^2(\mathbb{R})$ that generate wavelet bases. The Fourier transform maps the admissible wavelets to the set $\hat{\mathfrak{A}}$ containing functions: 1) that satisfy the wavelet admissibility condition $G \in K_1(\mathbb{R})$ and 2) whose inverse Fourier transforms generate wavelet bases. The map Λ_c takes these Fourier transforms and warps them, yielding a function in the set $\hat{\mathfrak{B}}$. An inverse Fourier transform takes these resulting functions back to the time domain.

[3]Two vector spaces, $\mathfrak{X}$ and $\mathfrak{Y}$, are said to be *isomorphic* if there is a one-to-one, linear mapping T of $\mathfrak{X}$ onto $\mathfrak{Y}$ [11]. Two normed vector spaces, $\mathfrak{X}$ and $\mathfrak{Y}$, are *isometrically isomorphic* if they are isomorphic and if the corresponding mapping T is isometric; that is if $\|Tx\|_{\mathfrak{Y}} = \|x\|_{\mathfrak{X}}$, where $\|\cdot\|_{\mathfrak{U}}$ represents the norm in the space $\mathfrak{U}$.

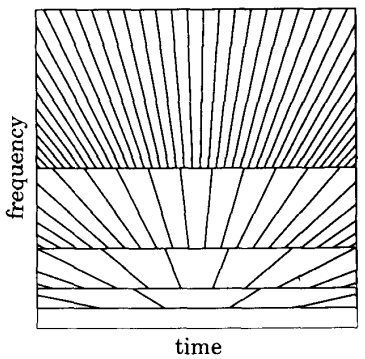

Fig. 2. Idealized tiling of the time-frequency plane by the elements $\{\boldsymbol{b}_{m,n}^{\text{fan}}\}$ of a fan orthonormal basis for the case $c = 2$ (linear chirp). The tiling is generated from a single, fixed wavelet function via scaling and shears in time.

Note, as a special case of Theorem 1, that Λ_c is unitary from $K_0(\mathbb{R}) = L^2(\mathbb{R})$ onto $K_0(\mathbb{R}) = L^2(\mathbb{R})$. Thus, if the set $\mathfrak{A}$ from the left side of (13) is expanded to all of $L^2(\mathbb{R})$, then the three-part operator isometrically and isomorphically links the following spaces:

$$L^2(\mathbb{R}) \xrightarrow{\boldsymbol{F}} L^2(\mathbb{R}) \xrightarrow{\Lambda_c} L^2(\mathbb{R}) \xrightarrow{\boldsymbol{F}^{-1}} L^2(\mathbb{R}). \tag{14}$$

This demonstrates that $\Theta_c = \boldsymbol{F}^{-1}\Lambda_c\boldsymbol{F}$ is unitary on $L^2(\mathbb{R})$.

C. Fan Bases from Wavelet Bases

An important property of an isometric isomorphism is that it maps orthonormal bases to orthonormal bases. Thus, if we apply the operator Θ_c to the elements of an arbitrary wavelet basis for $L^2(\mathbb{R})$, the result will be another basis for $L^2(\mathbb{R})$. It is easy to see that the application of Θ_c to an arbitrary wavelet basis yields the fan basis of (7) and (8); that is, we have

$$\boldsymbol{b}_{m,n}^{\text{fan}}(t) = (\Theta_c \boldsymbol{b}_{m,n}^{\text{wavelet}})(t) \tag{15}$$

if we make the correspondences $g_{\text{fan}} = \Theta_c g_{\text{wavelet}}$, $p_0 = t_0$, and $r_0 = a_0^{1/c}$. Hence, every wavelet orthonormal basis for $L^2(\mathbb{R})$ can be mapped into an equivalent fan orthonormal basis of order c for $L^2(\mathbb{R})$ simply by applying the unitary operator Θ_c to the wavelet g_{wavelet} generating the wavelet basis and then employing (8). Furthermore, this procedure generates *all* fan bases of all orders. This follows from the fact that the inverse of the three-part operator, $\Theta_c^{-1} = \boldsymbol{F}^{-1}\Lambda_c^{-1}\boldsymbol{F}$, is also unitary, and hence, it maps every fan basis to a wavelet one. We have thus proved the following fundamental result.

Theorem 2: The function g_{wavelet} generates an orthonormal wavelet basis for $L^2(\mathbb{R})$ with parameters a_0, t_0, if and only if the function g_{fan}, where $g_{\text{fan}} = \Theta_c g_{\text{wavelet}}$, generates an orthonormal fan basis of order $c \neq 0$ for $L^2(\mathbb{R})$ as in (8) with parameters $r_0 = a_0^{1/c}$ and $p_0 = t_0$.

Note that the sampling lattices of the two bases in the theorem are subtly different. Most conspicuous is the $r_0 = a_0^{1/c}$ spacing in scale in the fan bases (typically $a_0 = 2$ for a wavelet basis). In Fig. 3, we plot the warped function $\Theta_2 g$, with g a "Daubechies-2" wavelet [4]. This warped function, while no longer compactly supported[4], generates a valid fan basis of order 2.

[4]We do not know at present whether there exist compactly supported functions generating fan bases.

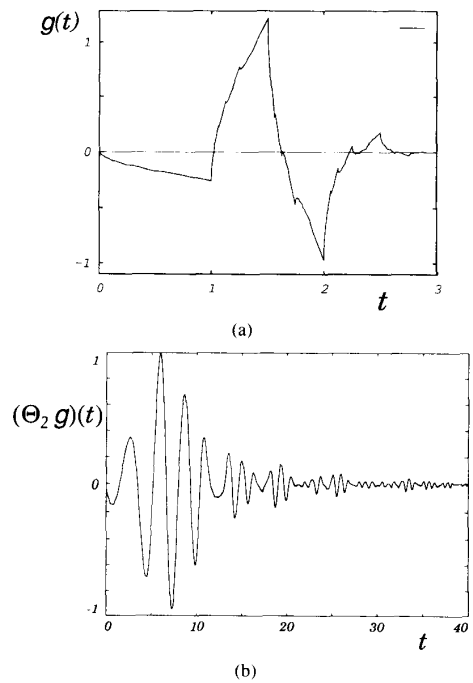

Fig. 3. (a) A "Daubechies-2" wavelet basis element g [4] and (b) a portion of the warped function $\Theta_2 g$. The function $\Theta_2 g$ generates a valid fan basis of order $c = 2$ when used in (8).

Note that since the set $\mathcal{B}$ in (13) signifies all functions g_{fan} that generate valid fan bases, the set $\hat{\mathcal{B}}$ represents an admissibility condition for these functions. This condition is $G_{\text{fan}} \in K_c(\mathbb{R})$. For the case $c = 2$, this condition is consistent with the admissibility condition derived for the continuous-valued scale-shear transform in [12].

The computation of the coefficients $c^{\text{fan}}_{m,n}$ for the fan basis expansion (1) appears cumbersome, but it can be efficiently implemented by again utilizing the special properties of the operator Θ_c. The isometry of this operator from $L^2(\mathbb{R})$ onto $L^2(\mathbb{R})$ allows us to compute the expansion coefficients by first "prewarping" the signal and then computing the wavelet basis coefficients:

$$\begin{aligned} c^{\text{fan}}_{m,n} &= \langle s, \boldsymbol{b}^{\text{fan}}_{m,n} \rangle \\ &= \langle \Theta_c^{-1} s, \Theta_c^{-1} \boldsymbol{b}^{\text{fan}}_{m,n} \rangle \\ &= \langle \Theta_c^{-1} s, \boldsymbol{b}^{\text{wavelet}}_{m,n} \rangle. \end{aligned} \tag{16}$$

While indicating that the fan basis expansion can be implemented just as efficiently (modulo the prewarping) as the original wavelet basis expansion, this computation also emphasizes the dual interpretation that warping a basis set to match a signal is equivalent to prewarping the signal to match the original basis. Efficient computation of the prewarped signal $\Theta_c^{-1} s$ should be possible using techniques analogous to the fast Mellin transform, which requires a geometric scaling of the transform axis [13]–[15].

III. Generalized Gabor and Wilson Bases: The Resetting Chevron Bases

A. Basis Elements

The mathematical machinery of the previous section can also be applied to the Gabor and Wilson bases. Since the axis warping operator Λ_c of (11) maps functions $z(v)$ that vary linearly in v to functions that vary in powers of v, application of Λ_c to a valid Gabor basis generates a basis with elements that employ chirp, rather than simply sinusoidal, modulation:

$$\begin{aligned} \boldsymbol{b}'_{m,n}(t) &= (\Lambda_c \boldsymbol{b}^{\text{Gabor}}_{m,n})(t) \\ &= |c|^{1/2} |t|^{(c-1)/2} g_{\text{Gabor}}(|t|^c \operatorname{sign}(t) - nt_0) \\ &\quad \cdot \exp[j2\pi m f_0 |t|^c \operatorname{sign}(t)]. \end{aligned} \tag{17}$$

However, while the set $\{\boldsymbol{b}'_{m,n}\}$ is an orthonormal basis for $L^2(\mathbb{R})$, the shape of the function in front of the exponential changes with each value of n, and thus, this basis cannot be built from simple translates and chirp modulates of a single, fixed window function. This limitation results because the action of the time shift by nt_0 does not commute with the action of Λ_c. Therefore, in the next section, we will modify the structure of Λ_c to construct a new axis warping operator whose action does commute with time shifts.

The result is a family of *resetting* shift-shear bases. Taking $t_0 = 1$ (without loss of generality), the elements of the order c resetting shift-shear basis derived from a Gabor basis are given by

$$\boldsymbol{b}^{\text{Greset}}_{m,n}(t) = g_{\text{Greset}}(t - n) \exp[j2\pi m q_0((t - \lfloor t \rfloor)^c + \lfloor t \rfloor)], \quad c \in \mathbb{R}, c \neq 0. \tag{18}$$

The term "resetting" is used to indicate that the instantaneous frequency of the chirp modulation is reset to zero at every integer along the time axis. The time-frequency plane tiling for an idealized Gabor shift-shear basis is shown in Fig. 4 for the case $c = 2$ (linear chirp). Because of the "V" shape of the basis tiling, we will refer to these bases as (resetting) *chevron* bases. Note, that in contrast to the scale-shear fan bases, which utilize convolution with chirp functions to shear in the time direction in the time-frequency plane, the chevron bases shear in the frequency direction by chirp modulation. However, like the fan bases, the tilting elements of the chevron bases could prove useful for efficiently representing chirp signals.

B. The Resetting Axis Warping Operator Υ_c

We now demonstrate that the Gabor resetting chevron bases of (18) are valid orthonormal bases for $L^2(\mathbb{R})$. We begin by modifying the axis warping operator Λ_c of Section II.

Definition 2: The *resetting axis warping operator* Υ_c is given by

$$(\Upsilon_c z)(u) = |c|^{1/2} (u - \lfloor u \rfloor)^{(c-1)/2} z((u - \lfloor u \rfloor)^c + \lfloor u \rfloor), \quad c \in \mathbb{R}, c \neq 0. \tag{19}$$

The inverse resetting axis warping operator is

$$(\Upsilon_c^{-1} z)(u) = |c|^{-1/2} (u - \lfloor u \rfloor)^{(1-c)/2c} z((u - \lfloor u \rfloor)^{1/c} + \lfloor u \rfloor). \tag{20}$$

The effect of Υ_c is to periodically (between each integer) warp the scale of the function z and multiply it by a periodic $u^{(c-1)/2}$ window. Fig. 5 illustrates the effect of Υ_2 on the Gabor basis element $\boldsymbol{b}^{\text{Gabor}}_{4,0}$, which was computed using the window constructed in [7] for g_{Gabor}. In this case, Υ_2 warps the single sinusoid to resetting chirp functions. The resetting axis warping operator shares a key property with its cousins Λ_c and Θ_c.

Theorem 3: The resetting axis warping operator Υ_c is unitary from $L^2(\mathbb{R})$ onto $L^2(\mathbb{R})$ for all $c \in \mathbb{R}$, $c \neq 0$.

The proof is very similar to that for Theorem 1 and is therefore omitted.

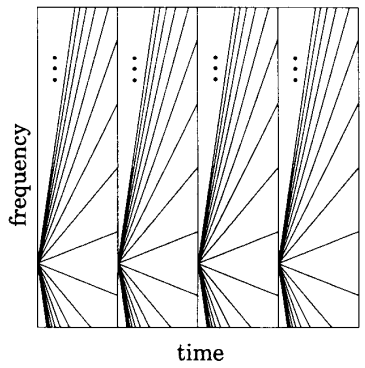

Fig. 4. Idealized tiling of the time–frequency plane by the elements $\{b_{m,n}^{\text{Greset}}\}$ of a (Gabor) resetting chevron orthonormal basis for the case $c = 2$ (linear chirp). The tiling is generated from a single, fixed window function via translations in time and shears in frequency.

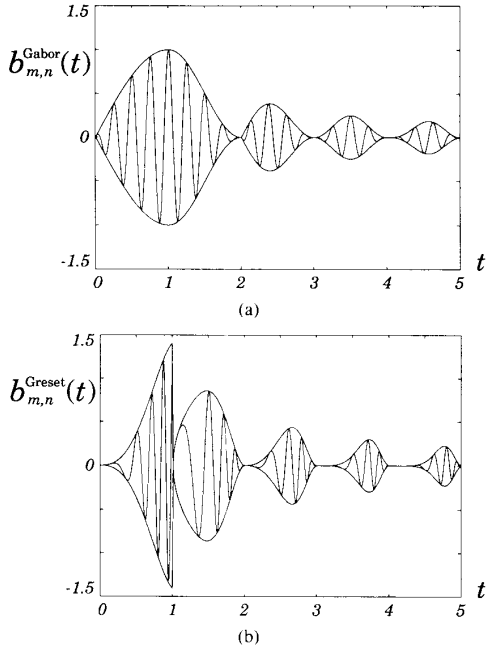

Fig. 5. The resetting axis warping operator Υ_2 applied to the Gabor basis element $b_{4,0}^{\text{Gabor}}(t) = g(t)e^{j8\pi t}$, where g is the window function constructed in [7]. (a) Real part of the Gabor basis element $b_{4,0}^{\text{Gabor}}(t)$. (b) Real part of the resetting chevron basis element $b_{4,0}^{\text{Greset}}(t) = (\Upsilon_2 b_{4,0}^{\text{Gabor}})(t)$.

C. Resetting Chevron Bases from Gabor and Wilson Bases

We can infer from Theorem 3 that Υ_c maps each orthonormal basis for $L^2(\mathbb{R})$ to another orthonormal basis for $L^2(\mathbb{R})$. Furthermore, it is simple to show that the application of Υ_c to an arbitrary Gabor basis yields a resetting chevron basis of the form (18); that is, we have

$$b_{m,n}^{\text{Greset}}(t) = (\Upsilon_c b_{m,n}^{\text{Gabor}})(t) \tag{21}$$

if we make the correspondences $g_{\text{Greset}} = \Upsilon_c g_{\text{Gabor}}$ and $q_0 = f_0$. Thus, every Gabor orthonormal basis can be mapped into an equivalent resetting chevron orthonormal basis of order c (and vice versa) simply by applying the unitary operator Υ_c to the window g_{Gabor} generating the Gabor basis and then employing (18). Furthermore, this procedure generates *all* chevron bases of all orders, since Υ_c^{-1} is also unitary and, hence, maps every resetting chevron basis to a Gabor one. The following theorem summarizes our results.

Theorem 4: The function g_{Gabor} generates an orthonormal Gabor basis for $L^2(\mathbb{R})$ with parameters $t_0 = 1$, $f_0 = 1$ if and only if the function g_{Greset}, where $g_{\text{Greset}} = \Upsilon_c g_{\text{Gabor}}$, generates an orthonormal resetting chevron basis of order $c \neq 0$ for $L^2(\mathbb{R})$ as in (18) with parameters $t_0 = 1$, $q_0 = 1$.

Note, that while we have emphasized the Gabor case up to this point, the operator Υ_c can also be used to construct families of resetting chevron bases from the Wilson bases [10] in exactly the same fashion.

IV. Regularity of the New Bases

It has been demonstrated recently that the *regularity* of the wavelet/window is an important performance criterion for a basis, since the degree of regularity controls the extent to which errors in the basis expansion coefficients are propagated into the resulting signal expansion (1) [4], [16], [17]. Roughly speaking, if a function has a regularity order of α, then it possesses at least $\lfloor \alpha \rfloor$ continuous derivatives. There are several different definitions of regularity order; see [16], [17] for more details.

Since the fan bases are constructed by applying the axis warping operator Λ_c in the frequency domain to the Fourier transform of a wavelet g_{wavelet}, we will find the following definition most convenient for results on these bases.

Definition 3: A function g has *Sobolev regularity order* $\alpha - 1/2$ if the function $f^{\alpha} G(f) \in L^2(\mathbb{R})$, where G is the Fourier transform of g.

Now, the simple structure of Λ_c leads directly to a fundamental result.

Theorem 5: Let g_{wavelet} be a function of Sobolev regularity order $\alpha - 1/2$. Then, the Sobolev regularity order of the function $g_{\text{fan}} = \Theta_c g_{\text{wavelet}}$ is $c\alpha - 1/2$.

Proof: We must show that the function $f^{c\alpha}(\Lambda_c G_{\text{wavelet}})(f) \in L^2(\mathbb{R})$. Using the definition of Sobolev regularity and the change of variable $u = |f|^c \operatorname{sign}(f)$, we have

$$\begin{aligned}\int |f^{c\alpha}(\Lambda_c G_{\text{wavelet}})(f)|^2 \, df &= \int |f|^{2c\alpha} |c|^{1/2} |f|^{(c-1)/2} \\ &\quad \cdot G_{\text{wavelet}}(|f|^c \operatorname{sign}(f))|^2 \, df \\ &= \int |u^{\alpha} G_{\text{wavelet}}(u)|^2 \, du. \end{aligned} \tag{22}$$

Since the regularity order of g_{wavelet} is $\alpha - 1/2$, this last term is finite, and the result follows. □

This result demonstrates that fan bases of order $c > 1$ are *more* regular than the original wavelet bases from which they were derived. This is due to the fact that, for $c > 1$, the frequency axis warp Λ_c compresses the wavelet function in the frequency domain, reducing the high frequency content of the resulting time domain function g_{fan} and thus making it smoother.

Unfortunately, a similar result does not hold for the resetting chevron bases. In particular, the warped window g_{reset} constructed by the application of the resetting axis warping operator Υ_c to a Gabor or Wilson window function cannot be continuous (see Fig. 5(b), for example). The source of the problem is the multiplication by the resetting window function $(u - \lfloor u \rfloor)^{(c-1)/2}$ in (19). This function, while highly regular between integers, is discontinuous at each integer. However, we note that while this lack of regularity will limit the resulting time and shear bases to applications where smoothness is not a prerequisite, this is already somewhat the case

for the Gabor bases, since if a window g generates a Gabor basis, then either g or its Fourier transform G is not continuously differentiable.[5]

V. Conclusions

The proportional-bandwidth and constant-bandwidth signal decompositions of the wavelet, Gabor, and Wilson bases have attracted substantial interest recently for representing signals with time-varying frequency content. However, these representations are also limited in that they are based on a rectangular tessellation of the time-frequency plane. Since few tools have been developed for dealing with the signal classes for which these tilings are ill suited, we have explored in this paper some simple nonrectangular time-frequency tilings. The most striking feature of the new scale-shear fan bases (8) and the shift-shear resetting chevron bases (18) is that they represent signals completely in terms of chirp functions. While the creation of the two new time–frequency plane tilings in Figs. 2 and 4 is theoretically interesting, these new bases may also be useful for representing certain types of signals, such as chirping and dispersed signals.

Our approach in deriving these two new classes of bases was to "bootstrap" the existing wavelet, Gabor, and Wilson basis theory to the problem at hand via the special axis warping operators Λ_c and Υ_c. In the fan basis case, this approach proved remarkably successful, resulting in a class of bases that not only have the correct form, but also have improved regularity properties over the wavelet bases from which they were derived. In the chevron basis case, this approach proved somewhat less successful. To arrive at a set of bases generated by only translations and chirp modulations, we were forced to modify the warping operator Λ_c to the resetting axis warping operator Υ_c. Unfortunately, the resetting operator is not sufficiently smooth to preserve the regularity properties of the Gabor or Wilson bases, and the resulting resetting chevron bases are at best only almost continuous.

The existence of an isometric isomorphism between the fan bases and the wavelet bases is no doubt due to the strong connection between their underlying group structures—the group that spawns the scale-shear fan transform [12] is isomorphic to the scalar affine group that spawns the wavelet transform [1]. On the other hand, the lack of strong connections between Gabor bases, which are generated by the Weyl-Heisenberg group [1], an the Wilson and chevron bases, which are not generated by any group, makes it more understandable why the application of axis warping operators to the Gabor and Wilson bases did not create completely satisfying chevron bases.

Note that several of the bases we have considered can be related to a discretization of the *metaplectic transform*, a new transform introduced in [19], [20] and studied further in [12]. In the wavelet and Gabor bases, the transformations applied to the wavelet/window are limited to time–frequency translation and time–frequency scaling. The five-dimensional metaplectic transform, on the other hand, is constructed to implement a general 2×2 unimodular, affine transformation, $Ax + b$, $|A| = 1$, in the time-frequency plane. The extra degrees of freedom in this transformation allow basis elements to not only translate and scale in time–frequency, but also to shear and rotate. It is shown in [12] that the wavelet, Gabor, and fan bases ($c = 2$ case) correspond to discretizations of the metaplectic transform along certain two-dimensional planes of its five-dimensional analysis space.

[5]This fact follows directly from Definition 3 and the *Balian-Low Theorem*, which states that if a window g generates a Gabor basis, then either $tg(t) \notin L^2(\mathbb{R})$ or $fG(f) \notin L^2(\mathbb{R})$ [6], [18].

Finally, besides the development of a more general theory for nonrectangular time-frequency tilings, this paper leaves many questions unanswered. We have not considered chirp basis decompositions for discrete-time signals. One potential problem with discrete-time signals is that a chirp signal will eventually violate the Nyquist criterion and alias. However, there could exist discrete-time bases that actually take advantage of this aliasing property. Another interesting research direction is the application of more general unitary operators for warping bases. Since every unitary transformation maps a basis set to another basis set, there seems to be no reason to stop with the two axis warping operators employed in this paper. This approach is adopted in [21], [22], where it is shown that unitary transformations provide a simple means for matching basis sets to particular classes of signals.

Acknowledgments

The authors wish to thank Olivier Rioul for helpful discussions about regularity, Brian Usevitch for creating the Daubechies wavelet plot in Fig. 3(a), Adrienne Samuels for reading the manuscript, and the reviewers for suggesting useful additions. This work was supported by the Sound Group of the Computer-based Education Research Laboratory at the University of Illinois, an NSERC-NATO postdoctoral fellowship, the Joint Services Electronics Program, Grant No. N00014-90-J-1270, and the National Science Foundation, Grant No. MIP 90-12747.

References

[1] C. Heil and D. Walnut, "Continuous and discrete wavelet transforms," *SIAM Rev.*, vol. 31, pp. 626–666, Dec. 1989.

[2] I. Daubechies, "The wavelet transform, time-frequency localization and signal analysis," *IEEE Trans. Inform. Theory*, vol. 36, pp. 961–1005, Sept. 1990.

[3] H. Feichtinger and K. Gröchenig, "Banach spaces related to square integrable group representations and their atomic decompositions I," *J. Functional Anal.*, vol. 86, pp. 307–340, 1989.

[4] I. Daubechies, "Orthonormal bases of compactly supported wavelets," *Commun. Pure Appl. Math.*, vol. XLI, pp. 909–996, 1988.

[5] D. Gabor, "Theory of communication," *J. IEE*, vol. 93, pp. 429–457, 1946.

[6] R. Balian, "Un principe d'incertitude fort en théorie du signal on en mécanique quantique," *Comptes Rendus de l'Academie des Sciences*, Paris, vol. 292, Série II, pp. 1357–1362, June 1, 1981.

[7] H. E. Jensen, T. Høholdt, and J. Justesen, "Double series representation of bounded signals," *IEEE Trans. Inform. Theory*, vol. IT-34, pp. 613–624, 1988.

[8] R. Tolimieri and R. Orr, "Poisson summation, the ambiguity function, and the theory of Weyl-Heisenberg frames," *IEEE Trans. Inform. Theory*, preprint.

[9] R. Coifman, Y. Meyer, and V. Wickerhauser, *Wavelet Analysis and Signal Processing*. New Haven, CT: Yale University Press, 1991.

[10] I. Daubechies, S. Jaffard, and J.-L. Journé, "A simple Wilson basis with exponential decay," *SIAM J. Math. Anal.*, vol. 22, pp. 554–572, Mar. 1991.

[11] D. G. Luenberger, *Optimization by Vector Space Methods*. New York: Wiley, 1969.

[12] R. G. Baraniuk, "Shear madness: Signal-dependent and metaplectic time–frequency representations," Coordinated Science Laboratory, University of Illinois at Urbana-Champaign, Tech. Rep., no. UILU-ENG-92-2226, 1992.

[13] J. Bertrand, P. Bertrand, and J. P. Ovarlez, "Discrete Mellin transform for signal analysis," in *Proc. ICASSP '90*, 1990, pp. 1603–1606.

[14] J. P. Ovarlez, J. Bertrand, and P. Bertrand, "Computation of affine time-frequency distributions using the fast Mellin transform," in *Proc. ICASSP '92*, pp. V117–V120, 1992.

[15] J. C. Allen, "Truncated sampling for the Fourier-Mellin transform with applications to wide-band WVD computation," in T. Luk, Ed. *Advanced Signal Processing Algorithms, Architectures and Implementations*, vol. Proc. SPIE-1348, pp. 279–290, 1990.

[16] O. Rioul, "Simple, optimal regularity estimates for wavelets," in *13ème Colloque GRETSI*, pp. 937-940, Sept. 1991.
[17] ——, "Simple regularity criteria for subdivision schemes," *SIAM J. Math. Anal.*, vol. 23, pp. 1544-1576, Nov. 1992.
[18] G. Battle, "Heisenberg proof of the Balian-Low theorem," *Letters on Mathematical Physics*, vol. 15, pp. 175-177, 1988.
[19] S. Mann and S. Haykin, "The chirplet transform—a generalization of Gabor's logon transform," in *Vision Interface '91*, Calgary, Alberta, Canada, 1991.
[20] R. G. Baraniuk and D. L. Jones, "New dimensions in wavelet analysis," in *Proc. ICASSP '92*, pp. V137-V140, 1992.
[21] ——, "Warped wavelet bases: Unitary equivalence and signal processing," in *Proc. ICASSP '93*, vol. III, 1993, pp. 320-323.
[22] ——, "Unitary equivalence: A new twist on signal processing," *IEEE Trans. Signal Processing*, 1993, submitted.

Signal Reconstruction from Modified Auditory Wavelet Transform

Toshio Irino and Hideki Kawahara

***Abstract*—We propose a new method for signal modification in auditory peripheral representation: an auditory wavelet transform and algorithms for reconstructing a signal from a modified wavelet transform. We present the characteristics of signal analysis, synthesis, and reconstruction and also the data reduction criteria for signal modification.**

I. Introduction

The study of auditory function requires investigation of the role of various features observed in auditory peripheral representation. Thus we want to develop a signal modification method that provides signal analysis for constructing a representation simulating the actual human auditory periphery and provides a scheme for synthesizing signals that can be used in psychophysical experiments. The short-time Fourier transform (STFT) is widely used in the analysis and synthesis of signals represented on a linear frequency axis [1]. In addition to the constant-window STFT, filters like the rectangular filter can be defined for analysis and synthesis. The STFT and these filters, however, cannot satisfy the first requirement (1). And although several models simulating the human auditory periphery have been proposed [2] they cannot satisfy the second requirement because they do not provide a scheme for synthesizing signals from the representation. In this paper, we propose the use of the wavelet transform (WT) [3], [4] which simulates the characteristics of the auditory periphery when the analyzing wavelet is properly selected from the impulse response of an auditory model. The auditory wavelet transform (AWT) enables a representation of the auditory periphery to be constructed by analyzing signals, and it enables signals to be synthesized from the representation. "Granular analysis" [5] is a similar analysis and synthesis technique proposed for use in speech processing, but the AWT provides a representation more similar to the actual auditory filter and is applicable to the following reconstruction algorithm based on the wavelet transform theory.

Although a modified signal can be synthesized from the modified wavelet coefficients, the modification is restricted to manipulation of the wavelet magnitude coefficients because phase modification tends to cause unexpected results. In addition, it is difficult to determine the phase coefficients in such modification as nonuniform time-scaling and partial replacement of wavelet coefficients with other ones. It is, therefore, essential to develop a method for determining the phase or for reconstructing a signal from only the magnitude. Thus, we apply algorithms developed for the short-time Fourier transform [6]–[9] to reconstruct a signal from its modified wavelet transform coefficients, especially from their magnitude. Iterative reconstruction from magnitude information may increase the variability of signal modification.

An algorithm using the wavelet transform and the convex projection method has been proposed to demonstrate minimal information loss along the auditory pathway [10]. Although the convex function method enables us to derive the wavelet coefficients from the reduced data, phase information is essential for synthesizing signal because the real wavelet transform is used in the first stage. An algorithm for reconstructing a signal from only the wavelet magnitude coefficients should thus be developed as an extension of the wavelet transform. And for investigating such auditory characteristics as the time-frequency resolution, it is also important to provide signal modification scheme that operates on the reduced data.

II. Auditory Wavelet Transform

A. Wavelet Transform

Let us begin with an overview of the wavelet transform. For a signal $x(l)$, an arbitrary analyzing wavelet $\varphi(m)$ (which satisfies the admissibility conditions), scaling factors a_n, and shift factors b_{nj} for each wavelet are defined as

$$\varphi_{n,j}(m) = a_n^{-1/2}\varphi((m - b_{nj})/a_n) \tag{1}$$

where $a_n = \alpha^n$ and where $b_{nj} = a_n \beta j$ for Nyquist sampling or $b_{nj} = j$ for every sampling point corresponding to the signal $x(l)$. In this note, each wavelet has all sampling points ($b_{nj} = j$). The discrete wavelet transform is defined as

$$X(n, j) = p(n) \sum_{m=-\infty}^{\infty} \varphi^*_{n,j}(m)x(m) \tag{2}$$

where $p(n)$ is the output multiplier for each filter. If $p(n) = a_n^{-1/2}$, the output power of each filter is the same. The inverse wavelet transform is

$$x(l) = C^{-1} \sum_{n=-j}^{\infty} \sum_{j=-\infty}^{\infty} X(n, j)\varphi_{n,j}(l)/p(n) \tag{3}$$

where C^{-1} is a constant value calculated from the Fourier transform of the analyzing wavelet.

B. Cochlear Model

The model used in this paper consists of a middle ear filter and a cochlear model. The middle ear filter, for impedance matching, is a 12-dB/oct high-pass filter with cutoff frequency of 1.5 kHz. The cochlear response is given as the result of a one-dimensional fluid dynamics difference equation [11]–[13]. The distributed resistance in the cochlear model is chosen to be one-tenth (1/10) of

Manuscript received August 27, 1992; revised May 7, 1993. The Guest Editor coordinating the review of this paper and approving it for publication was Dr. Takao Nishitani.

I. Toshio is with NTT Basic Research Laboratories, Tokyo 180, Japan.
K. Hideki is with ATR Human Information Processing Laboratories, Kyoto 619-02, Japan.

IEEE Log Number 9212189.